Polypeptide-based amphiphilic brush copolymers as unimolecular micelles: synthesis, characterisation, and encapsulation study

Yukui Zheng, Miao Pan, Chao Lu, Daojun Liu ✉

Medical College, Shantou University, Shantou 515041, People's Republic of China
✉ *E-mail: liudj@stu.edu.cn*

Published in Micro & Nano Letters; Received on 13th March 2018; Revised on 26th April 2018; Accepted on 18th May 2018

Polypeptide-based amphiphilic brush copolymers PLL-*g*-(PBLG-*b*-PEG) and PLL-*g*-(PZLL-*b*-PEG) with a poly(L-lysine) (PLL) backbone and amphiphilic oligo(γ-benzyl-L-glutamate)-*b*-poly(ethylene glycol) (PBLG-*b*-PEG) or oligo(ε-benzyloxycarbonyl-L-lysine)-*b*-poly (ethylene glycol) (PZLL-*b*-PEG) side chains were synthesised, characterised, and evaluated as unimolecular nanocontainers to encapsulate hydrophobic guest molecules. The structure of these brush polymers was modulated by tuning the length of the PLL, PBLG/PZLL, and PEG segments. The final products were characterised with ^{1}H nuclear magnetic resonance and gel permeation chromatography. The morphology and aggregation behaviours of brush copolymers were examined by using a transmission electron microscope and dynamic light scattering. It was revealed that these water-soluble brush copolymers resembled unimolecular micelles in an aqueous solution. An encapsulation study was performed using pyrene and oil red O as the model compounds, and the results showed that hydrophobic molecules could be solubilised in these unimolecular micelles with high loading capacities. The synthesised polypeptide-based amphiphilic brush copolymers could serve as promising unimolecular nanocarriers for the delivery of hydrophobic drugs.

1. Introduction: Polymeric micelles with well-defined core–shell structures self-assembled from amphiphilic block copolymers have attracted extensive attention over the past decades because of their potential applications in drug delivery [1–3]. The hydrophobic core of polymeric micelles serves as a microreservoir to solubilise water-insoluble drugs, while the hydrophilic shell shields the core, protects the loaded drugs, and provides compatibility to the micelles with the aqueous environment. The structures of block copolymers can be widely modulated to impart the polymeric micelles with high drug loading, long-term circulation in vivo, sustained and/or controlled drug release, and enhanced permeability and retention effect, among others [1–3]. However, polymeric micelles suffer from poor stability in dilute environments, such as the bloodstream, and upon changes in temperature, ionic strength, and pH [4]. For example, when the concentration of block copolymers drops below the critical micelle concentration (CMC), the disassembly of micellar structures leads to a burst release of entrapped drugs before reaching the target tissues.

A wide variety of strategies, such as radical polymerisation, the addition of bifunctional crosslinkers, and disulphide bridges, have been employed to crosslink the pre-formed polymeric micelles to improve their stability [4]. The fabricated polymeric micelles crosslinked from the core, the waist, or the shell have demonstrated an improved stability upon dilution and stimuli-responsive disassembly behaviours [5–7]. An alternative strategy to enhance the stability of polymeric micelles is to construct unimolecular polymeric micelles, grafting a polymeric core (e.g. dendrimer, hyperbranched polymer, brush polymer, or cyclodextrins) with multiple star-shaped peripheral chains [8–10]. Such unimolecular polymeric micelles exhibit excellent stability against dilution because of the covalent linkage rather than intermolecular forces. These unimolecular micelles can be designed to encapsulate not only hydrophobic drugs but also hydrophilic guest molecules (anionic and cationic) through various host–guest interactions including hydrophobic interactions, electrostatic interactions, hydrogen bonding, host–guest recognition, and/or their combinations [11, 12]. On the other hand, drug molecules can also be chemically conjugated to the interior of the unimolecular micelles via labile linkages, therefore, enabling responsive drug release upon stimuli such as pH, a reducing agent, and temperature [13–15]. The peripheries of these unimolecular micelles could also be decorated with various functionalised groups with targeting and imaging properties to prepare multifunctional drug nanocarriers [16–18].

One particular requirement for the use of polymeric unimolecular micelles as drug delivery systems is their biocompatibility and biodegradability. To this end, hydrophobic biodegradable cores such as poly(L-lactide), poly(ε-caprolactone), poly(lactic-*co*-glycolic acid), poly(amino acid), and hydrophilic biocompatible shells such as poly(ethylene glycol) (PEG) have been used to construct polymeric micelles. Among these, polypeptides have attracted considerable attention because of their structural versatility, intrinsic biodegradability and bio-absorbability [19–21]. Recently, we reported the use of polypeptide-based star-block copolymers and brush copolymers as nanocarriers for the versatile and simultaneous encapsulation of hydrophobic and hydrophilic drugs [12, 22–24].

In this paper, we report the synthesis of polypeptide-based amphiphilic brush copolymers as unimolecular micelles for the encapsulation of water-insoluble molecules. The brush copolymers PLL-*g*-(PBLG-*b*-PEG) and PLL-*g*-(PZLL-*b*-PEG) are composed of a poly(L-lysine) (PLL) backbone and amphiphilic oligo(γ-benzyl-L-glutamate)-*b*-PEG (PBLG-*b*-PEG) or oligo(ε-benzyloxycarbonyl-L-lysine)-*b*-PEG (PZLL-*b*-PEG) side chains (Fig. 1). PEG is employed as the outer shell of the brush copolymer owing to its good water solubility, high degree of biocompatibility, and prolonged circulation time in the blood [25]. The structure of these brush copolymers was modulated by tailoring the length of each block in the brush. The aggregation behaviour of the brush copolymer was examined using dynamic light scattering (DLS). The encapsulation capacities of these brush copolymers towards poorly water-soluble guests were evaluated using pyrene and oil red O (OR) as model compounds.

2. Materials and methods

2.1. Materials: ε-Benzyloxycarbonyl-L-lysine (ZLL) and γ-benzyl-L-glutamate (BLG) were purchased from GL Biochem (Shanghai, China). Pyrene and OR were obtained from Alfa Aesar (Ward Hill, MA). Poly(ethylene glycol) monomethylethers (M_w = 2 and 5 kDa, denoted as PEG_{2k} and PEG_{5k}) and hexamethyldisilazane (HMDS) were obtained from Sigma-Aldrich (St. Louis, MO). Triphosgene, 4-nitrophenyl chloroformate

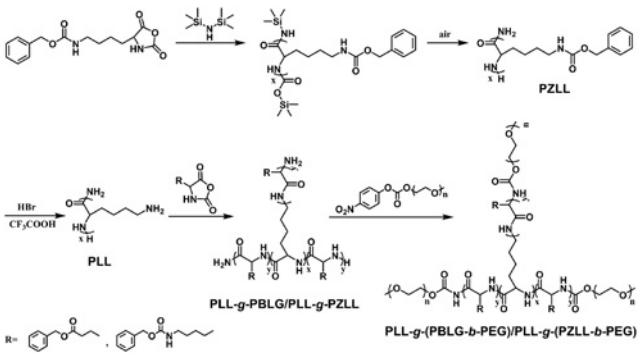

Fig. 1 *Synthesis of brush copolymers PLL-g-(PBLG-b-PEG) and PLL-g-(PZLL-b-PEG)*

(NPC), trifluoroacetic acid (TFA), triethylamine (TEA), and hydrogen bromide/acetic acid solution (HBr/CH_3COOH, 33%) were supplied by Aladdin (Shanghai, China). Dichloromethane (DCM), dimethyl sulfoxide (DMSO) and ethyl acetate were dried over CaH_2. Petroleum ether and tetrahydrofuran (THF) were dried by refluxing with sodium. Cellulose dialysis tubing with a molecular weight cut-off (MWCO) of 14 kDa was supplied by Viskase (Darien, IL). All of the other reagents were of analytical grade and were used as received.

2.2. Measurements: ^{1}H nuclear magnetic resonance (NMR) spectra were recorded on a Bruker DMX 400 MHz spectrometer using DMSO-d_6 or D_2O as a solvent. The molecular weight and molecular weight distributions were determined on a Waters 515 gel permeation chromatograph (GPC) equipped with a 2414 RI detector. $CHCl_3$ or 0.50 mol l^{-1} HAc-NaAc buffer (pH 4.5) was used as the eluent at a flow rate of 1 ml min^{-1} at 30°C, and the molecular weights were calibrated on poly(styrene) (PS) or PEG standards, respectively. UV–Vis absorption spectra were recorded on an UVPC 2501 spectrophotometer (Shimadzu).

2.3. Synthesis of PLL-*g*-(PBLG-*b*-PEG) and PLL-*g*-(PZLL-*b*-PEG): γ-Benzyl-L-glutamate *N*-carboxyanhydride (BLG-NCA), ε-benzyloxycarbonyl-L-lysine *N*-carboxyanhydride (ZLL-NCA), and PEG 4-nitrophenyl carbonate (PEG-NPC) were prepared according to the previously reported methods [24] and characterised by ^{1}H NMR.

The brush copolymers were prepared in four steps, as depicted in Fig. 1. (i) Poly(ε-benzyloxycarbonyl-L-lysine) (PZLL) was prepared by the ring-opening polymerisation (ROP) of ZLL-NCA initiated by HMDS. ZLL-NCA (2.5 g) was dissolved in 100 ml DCM, into which a given amount of HMDS solution in DCM (1.0×10^{-4} mol ml^{-1}) was added. The mixture was stirred under a N_2 atmosphere at room temperature for 24 h and then concentrated on a rotary evaporator to ~10, and 50 ml diethyl ether was subsequently poured to precipitate PZLL. The obtained PZLL was dried using a vacuum. (ii) The ε-benzyloxycarbonyl groups in PZLL were deprotected in the presence of HBr to produce poly(L-lysine) (PLL) following the reported method. Briefly, 1.0 g of PZLL was dissolved in 10 ml TFA, into which 1.5 ml HBr/CH_3COOH was added. The mixture was stirred at room temperature for 2 h and subsequently poured into 50 ml diethyl ether. The obtained PLL precipitates were rinsed thoroughly with diethyl ether under ultrasonic conditions and then dried using a vacuum. (iii) PLL was used as the macroinitiator to initiate the ROP of BLG-NCA or ZLL-NCA to produce the brush polymer poly(L-lysine)-*g*-poly-(γ-benzyl-L-glutamate) (PLL-*g*-PBLG) or poly(L-lysine)-*g*-poly (ε-benzyloxycarbonyl-L-lysine) (PLL-g-PZLL). For example, a given amount of BLG-NCA or ZLL-NCA was dissolved in the mixed solvents of 6 ml DCM and 3 ml DMSO, into which 0.02 g of PLL dissolved in 1.0 ml of DMSO was added, the mixture was stirred under a N_2 atmosphere at room temperature for 24 h. (iv) PEG was grafted to the periphery of PLL-*g*-PBLG or PLL-*g*-PZLL by reacting with PEG-NPC in the presence of TEA to obtain the final product PLL-*g*-(PBLG-*b*-PEG) or PLL-*g*-(PZLL-*b*-PEG). Briefly, DCM in the above reaction mixture was removed using a rotary evaporator, and 6 ml DMSO was added. A given amount of PEG-NPC and TEA were then added, and the mixture was stirred at 40°C for 7 days. After that, 10 ml of water was added, and the mixture was dialysed (MWCO 14 kDa) thoroughly against water for 5 days and lyophilised to obtain the final products. The final products and their intermediates were characterised with ^{1}H NMR and GPC.

2.4. Aggregation behaviour of PLL-*g*-(PBLG-*b*-PEG) and PLL-*g*-(PZLL-*b*-PEG): The brush copolymer solutions in both water and THF with a concentration of 5 mg ml^{-1} were prepared. The particle sizes of the polymer solutions were measured with a Brookhaven BI-200SM laser DLS system. The scattered light ($\lambda = 670$ nm) was detected at a 90° angle at room temperature and run in triplicate. The aggregation behaviour of the brush copolymers in the aqueous solution was then analysed by comparing the particle sizes within various solvents.

The morphologies of brush copolymers were visualised with a JEOL JEM-1400 transmission electron microscope (TEM) at an operating voltage of 120 kV. To prepare the samples, a drop of an aqueous solution of the brush copolymer (0.05 mg ml^{-1}) was deposited onto a carbon-coated copper grid. Excess copolymer solution was removed using a piece of filter paper, and the grid was dried under ambient atmosphere for 1 h.

2.5. Encapsulation of hydrophobic model compounds by PLL-*g*-(PBLG-*b*-PEG) and PLL-*g*-(PZLL-*b*-PEG): Three methods were employed to investigate the encapsulation of the brush copolymers towards hydrophobic model compounds pyrene and OR. (i) The brush copolymers were dissolved in deionised water at concentrations varying from 0.1 to 2.5 g l^{-1}, into which a pyrene/OR solution in DCM was added. The mixture was vigorously stirred for two days, and DCM was removed by rotary evaporation. (ii) The brush copolymers were dissolved in deionised water, into which pyrene/OR solid powder was added. The mixture was vigorously stirred for two days. (iii) The brush copolymers and model compounds were dissolved in DCM and stirred for 2 h; DCM was then removed by rotary evaporation. Deionised water was subsequently added, and the solution was vigorously stirred for 2 days. The insoluble dyes in all of the samples prepared by these three methods were removed by centrifugation at 14,000 rpm for 10 min, and the supernatant was analysed by a UV–Vis spectrophotometer. The amount of solubilised hydrophobic dyes was estimated in terms of the calibration curve of the model compounds in THF.

3. Results and discussion

3.1. Synthesis of PLL-*g*-(PBLG-*b*-PEG) and PLL-*g*-(PZLL-*b*-PEG): The designed brush copolymers have a PLL backbone and amphiphilic PBLG-*b*-PEG or PZLL-*b*-PEG side chains (Fig. 1). Their structures were modulated by tuning the respective length of PLL, PBLG, PZLL, and PEG blocks. The brush copolymers were prepared in four steps, as depicted in Fig. 1.

Firstly, PZLL was prepared by the ROP of ZLL-NCA initiated by HMDS. The ROP of amino acid-NCAs has been widely used for the preparation of various functional polypeptides. Traditional initiators for the ROP of amino acid-NCAs include primary amines and tertiary amines [26]. Later, controlled NCA polymerisation technologies were developed by Deming *et al.* using zero-valent nickel and cobalt as initiators to produce high molecular weight polypeptides [27]. Recently, Cheng *et al.* developed a simple and convenient approach for the controlled NCA

doi: 10.1049/mnl.2018.5094

polymerisation using organosilicon amines as initiators [28]. For instance, the molecular weights of polypeptides are excellently controlled with a very narrow distribution using HMDS as the initiator [28]. In the present study, the molar ratios of the ZLL-NCA monomer to the HDMS initiator were fixed at 100:1 and 200:1, therefore, $PZLL_{100}$ and $PZLL_{200}$ were expected to be produced as a result of the ROP of ZLL-NCA, where the subscripts 100 and 200 referred to the degree of polymerisation of PZLL. The resultant PZLL was characterised with ^{1}H NMR and GPC. The molecular weights of PZLL were measured with GPC using $CHCl_3$ as the eluent, the unimodal distribution of the GPC spectrum indicated that the synthesis proceeded in a controlled manner. The molecular weights of $PZLL_{100}$ and $PZLL_{200}$ obtained from the GPC measurements were 24.6 and 50.1 kDa, respectively, in accordance with the feeding ratios.

In the second step, the ε-benzyloxycarbonyl groups in PZLL were deprotected in the presence of HBr to produce PLL. The molecular weights of PLL_{100} and PLL_{200} were determined by GPC using a 0.50 mol l^{-1} HAc-NaAc buffer (pH 4.5) as the eluent. The obtained molecular weights for PLL_{100} and PLL_{200} were 11.4 and 23.1 kDa, respectively, consistent with the calculated values (12.8 and 25.6 kDa for PLL_{100} and PLL_{200}, respectively.)

In the third step, PLL was used as the macroinitiator to initiate the ROP of BLG-NCA or ZLL-NCA to produce the brush polymer PLL-*g*-PBLG or PLL-*g*-PZLL. The degree of polymerisation for PBLG and PZLL was varied from 2 to 4 and 6, therefore, 12 brush polymers PLL_{100}-*g*-$PBLG_2$, PLL_{100}-*g*-$PBLG_4$, PLL_{100}-*g*-$PBLG_6$, PLL_{200}-*g*-$PBLG_2$, PLL_{200}-*g*-$PBLG_4$, PLL_{200}-*g*-$PBLG_6$, PLL_{100}-*g*-$PZLL_2$, PLL_{100}-*g*-$PZLL_4$, PLL_{100}-*g*-$PZLL_6$, PLL_{200}-*g*-$PZLL_2$, PLL_{200}-*g*-$PZLL_4$, and PLL_{200}-*g*-$PZLL_6$ were expected to be produced after the polymerisation reaction, where 2, 4, and 6 referred to the degree of polymerisation for PBLG and PZLL side chains. Representative ^{1}H NMR spectra of PLL-*g*-PBLG and PLL-*g*-PZLL are shown in Figs. 2*a* and *b*. The molecular weights were determined by GPC using $CHCl_3$ as the eluent. The GPC chromatograms demonstrated a unimodal distribution. The molecular weights obtained from the GPC measurements (data not shown) were generally smaller than the calculated values, which is possibly due to the smaller hydrodynamic volume of brush polymers compared with the linear PS standard [15].

In the last step, PEG was grafted to the terminals of PBLG and PZLL to obtain the final product PLL-*g*-(PBLG-*b*-PEG) and PLL-*g*-(PZLL-*b*-PEG). The reaction between PLL-*g*-PBLG or PLL-*g*-PZLL and PEG-NPC was conducted in the presence of TEA as the catalyst. PEG with two molecular weights (2 and 5 kDa) was employed, and 18 final brush copolymers were obtained, PLL_{100}-*g*-($PBLG_2$-*b*-PEG_{2k}) (**P1**), PLL_{100}-*g*-($PBLG_4$-*b*-PEG_{2k}) (**P2**), PLL_{100}-*g*-($PBLG_6$-*b*-PEG_{2k}) (**P3**), PLL_{200}-*g*-($PBLG_2$-*b*-PEG_{2k}) (**P4**), PLL_{200}-*g*-($PBLG_4$-*b*-PEG_{2k}) (**P5**), PLL_{200}-*g*-($PBLG_6$-*b*-PEG_{2k}) (**P6**), PLL_{100}-*g*-($PZLL_2$-*b*-PEG_{2k}) (**P7**), PLL_{100}-*g*-($PZLL_4$-*b*-PEG_{2k}) (**P8**), PLL_{100}-*g*-($PZLL_6$-*b*-PEG_{2k}) (**P9**), PLL_{200}-*g*-($PZLL_2$-*b*-PEG_{2k}) (**P10**), PLL_{200}-*g*-($PZLL_4$-*b*-PEG_{2k}) (**P11**), PLL_{200}-*g*- ($PZLL_6$-*b*-PEG_{2k}) (**P12**), PLL_{100}-*g*-($PBLG_2$-*b*-PEG_{5k}) (**P13**), PLL_{100}-*g*-($PBLG_4$-*b*-PEG_{5k}) (**P14**), PLL_{100}-*g*-($PBLG_6$-*b*-PEG_{5k}) (**P15**), PLL_{200}-*g*-($PBLG_2$-*b*-PEG_{5k}) (**P16**), PLL_{200}-*g*-($PBLG_4$-*b*-PEG_{5k}) (**P17**), and PLL_{200}-*g*-($PBLG_6$-*b*-PEG_{5k}) (**P18**). Representative ^{1}H NMR spectra of **P3** and **P12** are shown in Figs. 2*c* and *d*. The appearance of the peak at ∼3.8 ppm indicated that PEG was successfully grafted. The molecular weights of the final products were examined by GPC using $CHCl_3$ as the eluent. Typical GPC chromatograms are shown in Fig. 3, and the results are listed in Table 1. Again, the molecular weights obtained from the GPC measurements were smaller than the theoretical values because of the smaller hydrodynamic volume of the brush polymers relative to the linear standard [17].

To illustrate the effect of the hydrophobic block, PBLG and PZLL, on the encapsulation capacity of the designed brush copolymers, two brush copolymers without interior hydrophobic blocks, PLL100-g-PEG2k (P19) and PLL200-g-PEG2k (P20), were also synthesised by directly grafting PEG to the PLL backbone. Their structures were confirmed by 1H NMR and GPC measurements (data not shown).

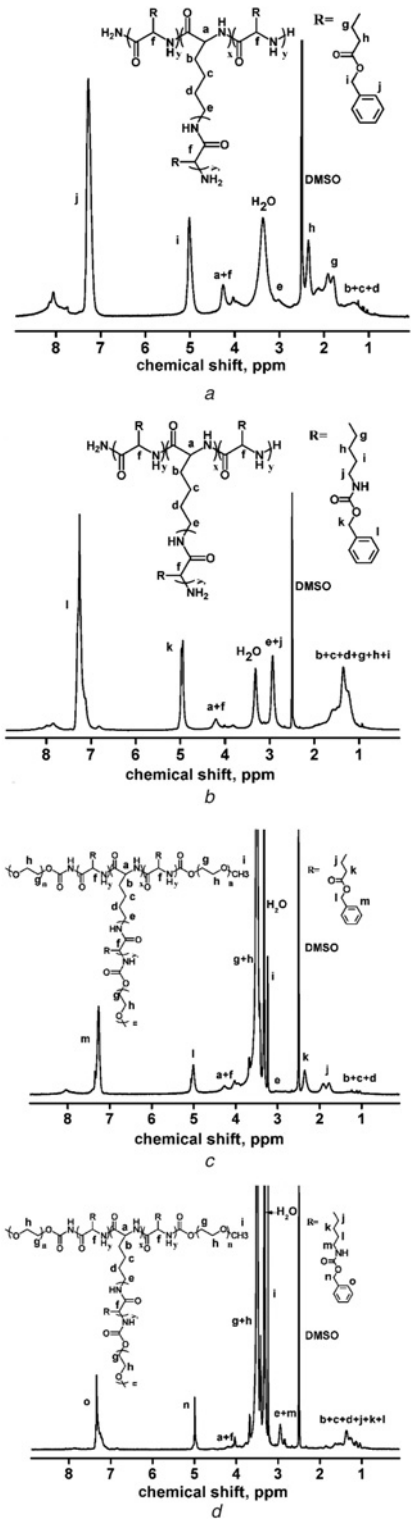

Fig. 2 *^{1}H NMR spectra of*
a PLL_{100}-*g*-$PBLG_4$
b PLL_{100}-*g*-$PZLL_4$
c **P3**
d **P12** in DMSO-d_6

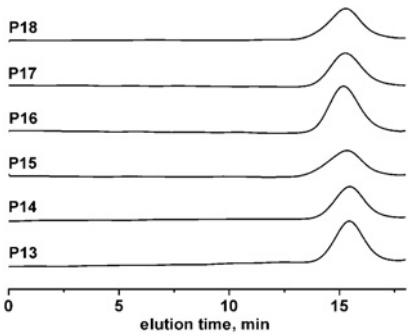

Fig. 3 *GPC chromatograms of PLL-g-(PBLG-b-PEG)*

3.2. Aggregation behaviour of PLL-*g*-(PBLG-*b*-PEG) and PLL-*g*-(PZLL-*b*-PEG): The synthesised brush copolymers possess a relatively long chain of the hydrophilic PEG periphery and a short length of the hydrophobic PBLG or PZLL inner block. The longer hydrophilic PEG outer shell prevented the aggregation of the brush polymers in the aqueous solution and is thus favourable for the formation of unimolecular micelles. To explore the aggregation behaviour of the synthesised brush copolymers in the aqueous solution, brush copolymer solutions with a concentration of up to 5 mg ml^{-1} were prepared in both THF and water, and the particle sizes were then determined using DLS. A high concentration of 5 mg ml^{-1} was chosen because it is generally much higher than the CMC of giant amphiphiles. It should be noted that the synthesised brush copolymers had a relatively small radial ratio, which might give rise to an approximately spherical shape rather than the cylindrical molecular geometry. The diameters of the individual brush copolymers with an extended chain conformation were estimated to be ∼30–60 nm, depending on the length of PLL, PZLL/PBLG, and PEG blocks. The particle sizes for **P13**, **P14**, **P15**, **P16**, **P17**, and **P18** obtained from DLS measurements in THF were 38, 40, 44, 51, 59, and 60 nm, respectively (Fig. 4*a*), in accordance with the sizes of the individual polymer molecules. As is well known, the present brush copolymers existed in the form of discrete molecules without aggregation in organic solvents, like THF. The sizes of the brush copolymers increased with the elongation of either the PLL backbone or the PBLG inner block. Notably, the particle sizes for the brush copolymers **P13**, **P14**, **P15**, **P16**, **P17**, and **P18** in water were 39, 44, 48, 46, 51, 65 nm, respectively (Fig. 4*b*), which are very close to the results obtained from the THF solutions. The DLS measurements for other brush copolymers gave similar diameters in THF and water. The approximate sizes for the brush copolymers in both THF and water, as well as their consistency with the theoretical diameter of the individual polymers, indicated that the synthesised brush copolymers were adopted as unimolecular polymeric micelles in the aqueous solution.

The morphologies of the brush copolymers were visualised by TEM and a typical TEM image is shown in Fig. 5. The polymer brushes adopted a spherical morphology which might be ascribed to the relatively smaller radial ratio again. As an example, the diameter of **P4** was 38 ± 8 nm, in accordance with the designed structure of the individual polymer brushes. The TEM results confirmed that the polymer brushes were prepared successfully and were well dispersed in the aqueous solution as unimolecular micelles.

3.3. Encapsulation of hydrophobic model compounds by PLL-*g*-(PBLG-*b*-PEG) and PLL-*g*-(PZLL-*b*-PEG): The synthesised brush copolymers PLL-*g*-(PBLG-*b*-PEG) and PLL-*g*-(PZLL-*b*-PEG) with a hydrophobic PBLG or PZLL interior and a hydrophilic PEG outer shell could serve as amphiphilic unimolecular nanocarriers to encapsulate non-polar guest molecules through hydrophobic interactions. Three encapsulation methods were compared to investigate the encapsulation of brush copolymers towards hydrophobic model compounds pyrene and OR. For the first method, pyrene or OR was encapsulated from a suspension of the polymer in a water and DCM mixture, while the solubilisation of solid pyrene or OR powder in the polymer aqueous solution was conducted in the second method. For the third method, pyrene or OR was entrapped by the brush copolymer in a DCM solution and then equilibrated in an aqueous solution. The results revealed that the loading capacity of the hydrophobic molecules in the brush polymer prepared from the first method was much lower than that of the latter two methods, and the loading capacity prepared from the third method was slightly higher than that from method 2. Therefore, the third method was

Table 1 Molecular weights and loading capacities of brush copolymers PLL-g-(PBLG-b-PEG) and PLL-g-(PZLL-b-PEG)

Polymer	Molecular weight, kDa		Loading capacity			
	Calc.	GPC (PDI)	$m_{pyrene}/m_{polymer}$, %	$n_{pyrene}/n_{polymer}$	$m_{OR}/m_{polymer}$, %	$n_{OR}/n_{polymer}$
PLL_{100}-*g*-($PBLG_2$-*b*-PEG_{2k}) (**P1**)	259.2	129.5 (1.12)	0.030	0.38	0.56	3.57
PLL_{100}-*g*-($PBLG_4$-*b*-PEG_{2k}) (**P2**)	303.0	154.3 (1.12)	0.032	0.48	0.71	5.26
PLL_{100}-*g*-($PBLG_6$-*b*-PEG_{2k}) (**P3**)	346.8	183.4 (1.10)	0.102	1.76	1.57	13.3
PLL_{200}-*g*-($PBLG_2$-*b*-PEG_{2k}) (**P4**)	518.4	309.7 (1.26)	0.025	0.65	0.38	4.81
PLL_{200}-*g*-($PBLG_4$-*b*-PEG_{2k}) (**P5**)	606.0	353.6 (1.29)	0.041	1.24	0.45	6.65
PLL_{200}-*g*-($PBLG_6$-*b*-PEG_{2k}) (**P6**)	693.4	374.5 (1.25)	0.074	2.54	0.80	13.6
PLL_{100}-*g*-($PZLL_2$-*b*-PEG_{2k}) (**P7**)	267.8	147.5 (1.13)	0.035	0.46	1.38	9.04
PLL_{100}-*g*-($PZLL_4$-*b*-PEG_{2k}) (**P8**)	320.2	169.6 (1.09)	0.032	0.51	1.23	9.66
PLL_{100}-*g*-($PZLL_6$-*b*-PEG_{2k}) (**P9**)	372.6	170.4 (1.10)	0.107	1.97	1.58	14.5
PLL_{200}-*g*-($PZLL_2$-*b*-PEG_{2k}) (**P10**)	535.6	223.5 (1.11)	0.030	0.77	1.02	13.4
PLL_{200}-*g*-($PZLL_4$-*b*-PEG_{2k}) (**P11**)	640.4	293.2 (1.12)	0.044	1.39	1.55	24.4
PLL_{200}-*g*-($PZLL_6$-*b*-PEG_{2k}) (**P12**)	745.2	348.2 (1.14)	0.102	3.79	1.60	29.2
PLL_{100}-*g*-($PBLG_2$-*b*-PEG_{5k}) (**P13**)	559.2	395.5 (1.42)	0.018	0.50	0.44	6.12
PLL_{100}-*g*-($PBLG_4$-*b*-PEG_{5k}) (**P14**)	603.0	382.4 (1.45)	0.024	0.73	0.77	11.5
PLL_{100}-*g*-($PBLG_6$-*b*-PEG_{5k}) (**P15**)	646.8	403.4 (1.46)	0.099	3.15	1.02	15.3
PLL_{200}-*g*-($PBLG_2$-*b*-PEG_{5k}) (**P16**)	1118	502.6 (1.45)	0.030	1.63	0.78	22.5
PLL_{200}-*g*-($PBLG_4$-*b*-PEG_{5k}) (**P17**)	1206	512.2 (1.50)	0.072	4.31	0.95	28.0
PLL_{200}-*g*-($PBLG_6$-*b*-PEG_{5k}) (**P18**)	1294	504.5 (1.48)	0.100	6.44	1.13	35.7
PLL_{100}-*g*-PEG_{2k} (**P19**)	212.8	110.8 (1.10)	0.016	0.17	0.25	1.34
PLL_{200}-*g*-PEG_{2k} (**P20**)	425.6	219.3 (1.12)	0.012	0.39	0.19	2.08

doi: 10.1049/mnl.2018.5094

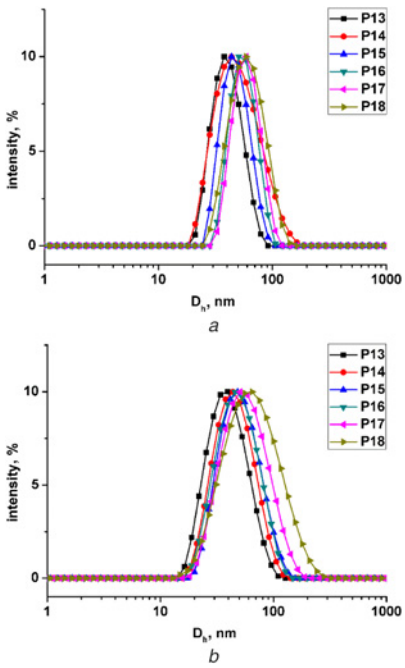

Fig. 4 *Hydrodynamic diameters (D_h) of PLL-g-(PBLG-b-PEG) in*
a THF
b Water, determined by DLS

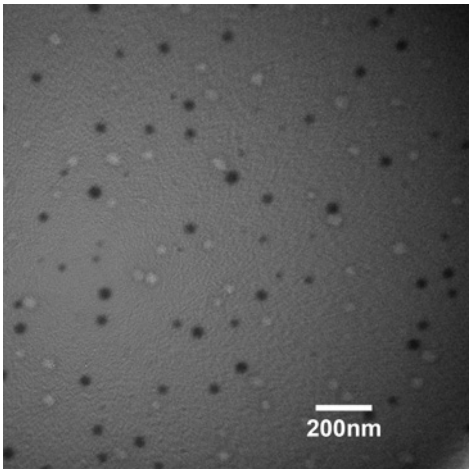

Fig. 5 *TEM image of **P4***

employed in the present study to investigate the loading capacity of the brush polymers towards pyrene and OR.

The amount of the encapsulated hydrophobic pyrene and OR increased in proportion to the concentration of PLL-*g*-(PBLG-*b*-PEG) and PLL-*g*-(PZLL-*b*-PEG) from 0.1 to 2.5 g l^{-1}. The solubilised pyrene exhibited a red-shift for the wavelength of maximum absorption (λ_{max}) from ~335 nm in pure water to ~340 nm in the presence of the polymers, which can be explained by the fact that pyrene molecules were located in the hydrophobic microenvironment created by the PBLG or PZLL inner blocks. The loading capacities of pyrene and OR, expressed as the mass ratio of guest molecules to the host polymers ($m_{guest}/m_{polymer}$), are listed in Table 1. The corresponding molar ratios ($n_{guest}/n_{polymer}$), which were estimated in terms of the theoretical molecular weight of PLL-*g*-(PBLG-*b*-PEG) and PLL-*g*-(PZLL-*b*-PEG), are also presented.

Generally, the loading capacities of hydrophobic guest molecules in the present brush copolymers are comparable to most reported drug delivery systems [2]. It can be shown from Table 1 that the loading capacity was a function of the structures of the block copolymers and model compounds. (i) The length of the PLL backbone had little effect on the loading capacity expressed in $m_{guest}/m_{polymer}$, which meant that the loading capacity expressed in $n_{guest}/n_{polymer}$ increased with the elongation of the PLL backbone. (ii) The elongation of the PBLG/PZLL block resulted in an increase in the loading capacity. It was noteworthy that the incorporation of the hydrophobic oligopeptide block into the brush copolymer was largely helpful for the solubilisation of water-insoluble guest molecules. The brush copolymers **P19** and **P20** without PZLL or PBLG blocks demonstrated poor encapsulation towards pyrene and OR, which also indicated that the water-insoluble guest molecules were predominantly entrapped by the PBLG/PZLL segments via hydrophobic interactions. (iii) The chemical nature of the hydrophobic inner block of the brush copolymers played an important role in the loading capacity. As shown, the brush copolymers with the PZLL inner block exhibited a higher encapsulation capacity compared with those of the copolymers with the PBLG inner block. (iv) An increase in the molecular weight of the peripheral PEG remarkably enhanced the loading capacity of the hydrophobic guest molecules. The unimolecular polymeric micelles might be well protected and stabilised by a longer PEG outer shell and thus were favourable for the encapsulation of water-insoluble guests. (v) The structures of the guest molecules also contributed to their loading capacities. The brush copolymers showed higher loading capacities for the larger OR molecules than the smaller pyrene. In summary, the loading capacity of hydrophobic guest molecules could be modulated by tailoring the structure of the polymeric unimolecular micelles, and a loading capacity of up to 1.6% could be realised. It should also be noted that the particle sizes of the PLL-*g*-(PBLG-*b*-PEG) and PLL-*g*-(PZLL-*b*-PEG) unimolecular micelles remained essentially the same after the encapsulation of pyrene or OR, as evidenced by the DLS measurements.

4. Conclusion: Two series of polypeptide-based brush copolymers, PLL-*g*-(PBLG-*b*-PEG) and PLL-*g*-(PZLL-*b*-PEG), with varying lengths of PLL, PBLG/PZLL, and PEG, were designed, synthesised, and characterised. DLS measurements revealed that these water-soluble brush polymers resembled unimolecular micelles in an aqueous solution. The encapsulation study demonstrated that hydrophobic model molecules pyrene and OR were encapsulated in these unimolecular micelles with high loading capacities. The biocompatibility, biodegradability, and high loading capacities made the synthesised brush copolymers promising unimolecular nanocarriers for the delivery of hydrophobic drugs.

5. Acknowledgments: This work was financially supported by the Department of Education, Guangdong Government under the Top-tier University Development Scheme for Research and Control of Infectious Diseases.

6 References

[1] Chao C., Jiang Y., Cheng R., *ET AL.*: 'Biodegradable polymeric micelles for targeted and controlled anticancer drug delivery: promises, progress and prospects', *Nano Today*, 2012, **7**, (5), pp. 467–480
[2] Gothwal A., Khan I., Gupta U.: 'Polymeric micelles: recent advancements in the delivery of anticancer drugs', *Pharm. Res.*, 2016, **33**, (1), pp. 18–39
[3] Li Z.-L., Huang Y.-S., Xiong X.-Y., *ET AL.*: 'Synthesis, characterisation and in vitro release of paclitaxel-loaded polymeric micelles', *Micro Nano Lett.*., 2017, **12**, (3), pp. 191–194
[4] Talelli M., Barz M., Rijchen C.-J.-F., *ET AL.*: 'Core-crosslinked polymeric micelles: principles, preparation, biomedical applications and clinical translation', *Nano Today*, 2015, **10**, (1), pp. 93–117

[5] Talelli M., Iman M., Varkouhi A.-K., *ET AL.*: 'Core-crosslinked polymeric micelles with controlled release of covalently entrapped doxorubicin', *Biomaterials*, 2010, **31**, (30), pp. 7797–7804
[6] Yuan C., Xu Y., Liao Y., *ET AL.*: 'Morphology tailoring and temperature sensitivity control of waist cross-linked micelles and evaluation of their application as intelligent drug carriers', *J. Mater. Chem.*, 2010, **20**, (44), pp. 9968–9975
[7] Yang R., Meng F., Ma S., *ET AL.*: 'Galactose-decorated cross-linked biodegradable poly(ethylene glycol)-*b*-poly(ε-caprolactone) block copolymer micelles for enhanced hepatoma-targeting delivery of paclitaxel', *Biomacromolecules*, 2011, **12**, (8), pp. 3047–3055
[8] Xu Z., Liu S., Liu H., *ET AL.*: 'Unimolecular micelles of amphiphilic cyclodextrin-core star-like block copolymers for anticancer drug delivery', *Chem. Commun.*, 2015, **51**, (87), pp. 15768–15771
[9] Cao W., Zhu L.: 'Synthesis and unimolecular micelles of amphiphilic dendrimer-like star polymer with various functional surface groups', *Macromolecules*, 2011, **44**, (6), pp. 1500–1512
[10] Zhang W., Li Y., Liu L., *ET AL.*: 'Amphiphilic toothbrushlike copolymers based on poly(ethylene glycol) and poly(ε-caprolactone) as drug carriers with enhanced properties', *Biomacromolecules*, 2010, **11**, (5), pp. 1331–1338
[11] Sun Y., Yan X., Yuan T., *ET AL.*: 'Disassemblable micelles based on reduction-degradable amphiphilic graft copolymers for intracellular delivery of doxorubicin', *Biomaterials*, 2010, **31**, (27), pp. 7124–7131
[12] Zeng X., Li J., Zheng J., *ET AL.*: 'Amphiphilic cylindrical copolypeptide brushes as potential nanocarriers for the simultaneous encapsulation of hydrophobic and cationic drugs', *Colloid Surf. B*, 2012, **94**, (7), pp. 324–332
[13] Johnson J.-A., Lu Y.-Y., Burts A.-O., *ET AL.*: 'Drug-loaded, bivalent-bottle-brush polymers by graft-through ROMP', *Macromolecules*, 2010, **43**, (24), pp. 10326–10335
[14] Yu Y., Chen C.-K., Law W.-C., *ET AL.*: 'Well-defined degradable brush polymer-drug conjugates for sustained delivery of paclitaxel', *Mol. Pharm.*, 2013, **10**, (3), pp. 867–874
[15] Yu Y., Chen C.-K., Law W.-C., *ET AL.*: 'Degradable brush polymer-drug conjugate for pH-responsive release of doxorubicin', *Polym. Chem.*, 2015, **6**, (6), pp. 953–961
[16] Guo J., Hong H., Chen G., *ET AL.*: 'Theranostic unimolecular micelles based on brush-shaped amphiphilic block copolymers for tumor-targeted drug delivery and positron emission tomography imaging', *ACS Appl. Mater. Interface*, 2014, **6**, (24), pp. 21769–21779
[17] Li X., Qian Y., Liu T., *ET AL.*: 'Amphiphilic multiarm star block copolymer-based multifunctional unimolecular micelles for cancer targeted drug delivery and MR imaging', *Biomaterials*, 2011, **32**, (27), pp. 6595–6605
[18] Chen G., Wang L., Cordie T., *ET AL.*: 'Multi-functional self-fluorescent unimolecular micelles for tumor-targeted drug delivery and bioimaging', *Biomaterials*, 2015, **47**, pp. 41–50
[19] Bae Y., Kataoka K.: 'Intelligent polymeric micelles from functional poly(ethylene glycol)-poly(amino acid) block copolymers', *Adv. Drug Deliv. Rev.*, 2009, **61**, (10), pp. 768–784
[20] Sun H., Meng F., Dias A.-A., *ET AL.*: 'α-Amino acid containing degradable polymers as functional biomaterials: rational design, synthetic pathway, and biomedical applications', *Biomacromolecules*, 2011, **12**, (6), pp. 1937–1955
[21] Lalatsa A., Schätzlein A.-G., Mazza M., *ET AL.*: 'Amphiphilic poly (L-amino acids)-new materials for drug delivery', *J. Controlled Release*, 2012, **161**, (2), pp. 523–536
[22] Zhuang W., Liao L., Chen H., *ET AL.*: 'Water soluble star-block copolypeptides: towards biodegradable nanocarriers for versatile and simultaneous encapsulation', *Macromol. Rapid Commun.*, 2009, **30**, (11), pp. 920–924
[23] Yan Y., Wei D., Li J., *ET AL.*: 'A poly(L-lysine)-based hydrophilic star block co-polymer as a protein nanocarrier with facile encapsulation and pH-responsive release', *Acta Biomater.*, 2012, **8**, (6), pp. 2113–2120
[24] Li J., Li J., Xu S., *ET AL.*: 'Hydrophobic oligopeptide-based star-block copolymers as unimolecular nanocarriers for poorly water-soluble drugs', *Colloid Surf. B*, 2013, **110**, (110C), pp. 183–190
[25] Wu H., Liu G., Zhang S., *ET AL.*: 'Biocompatibility, MR imaging and targeted drug delivery of a rattle-type magnetic mesoporous silica nanosphere system conjugated with PEG and cancer-cell-specific ligands', *J. Mater. Chem.*, 2011, **21**, (9), pp. 3037–3045
[26] Kricheldorf H.-R.: 'Polypeptides and 100 years of chemistry of α–amino acid N-carboxyanhydrides', *Angew. Chem. Int. Ed.*, 2006, **45**, (35), pp. 5752–5784
[27] Deming T.-J.: 'Synthesis and self-assembly of well-defined block copolypeptides via controlled NCA polymerization', *Adv. Polym. Sci.*, 2013, **262**, pp. 1–38
[28] Lu H., Cheng J.: 'Hexamethyldisilazane-mediated controlled polymerization of α-amino acid *N*-carboxyanhydrides', *J. Am. Chem. Soc.*, 2007, **129**, (46), pp. 14114–14115

doi: 10.1049/mnl.2018.5094